*Supplementary Materials*

# Facile and Sensitive Detection of Nitrogen-Containing Organic Bases with Near Infrared C-Dots Derived Assays

**Chunyu Ji [1], Yiqun Zhou [2], Wenquan Shi [1], Jiajia Wu [1], Qiurui Han [1], Tianshu Zhao [1], Roger M. Leblanc [2] and Zhili Peng [1,*]**

1. National Center for International Research on Photoelectric and Energy Materials, School of Materials and Energy, Yunnan University, Kunming 650091, China; jichunyu@mail.ynu.edu.cn (C.J.); shiwenquan1010@163.com (W.S.); 12019101477@mail.ynu.edu.cn (J.W.); hqr3155064793@163.com (Q.H.); zhaotianshu@mail.ynu.edu.cn (T.Z.)
2. Department of Chemistry, University of Miami, 1301 Memorial Drive, Coral Gables, FL 33146, USA; yxz431@miami.edu (Y.Z.); rml@miami.edu (R.M.L.)
3. Correspondence: zhilip@ynu.edu.cn; Tel.: +86–871–65037399

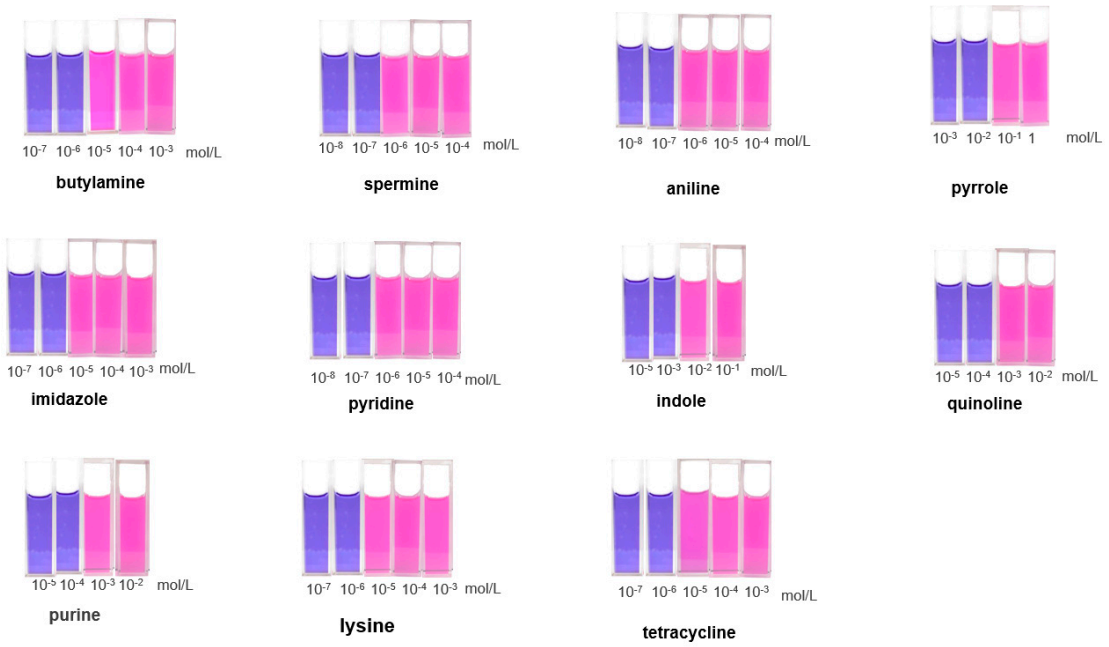


**Figure S1.** Solution assays for the detection of nitrogen-containing organic bases (NCOBs)

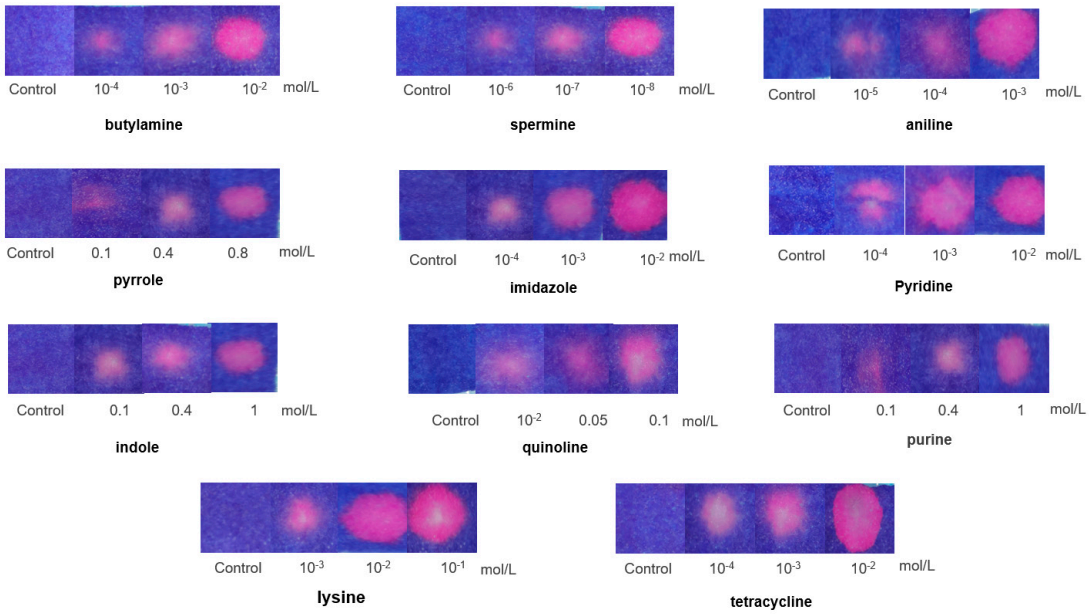


**Figure S2.** Test paper assays for the detection of NCOBs

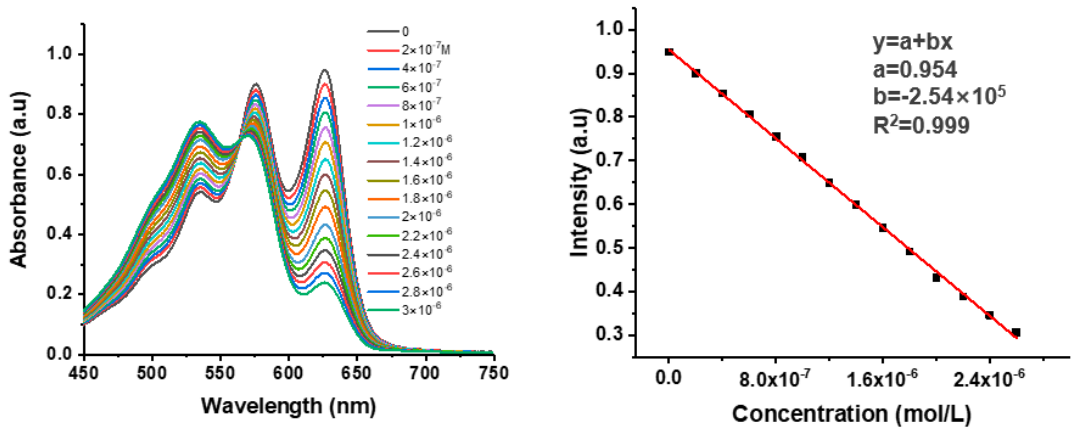


**Figure S3.** Detection of butylamine using UV-vis absorption-based sensing assay

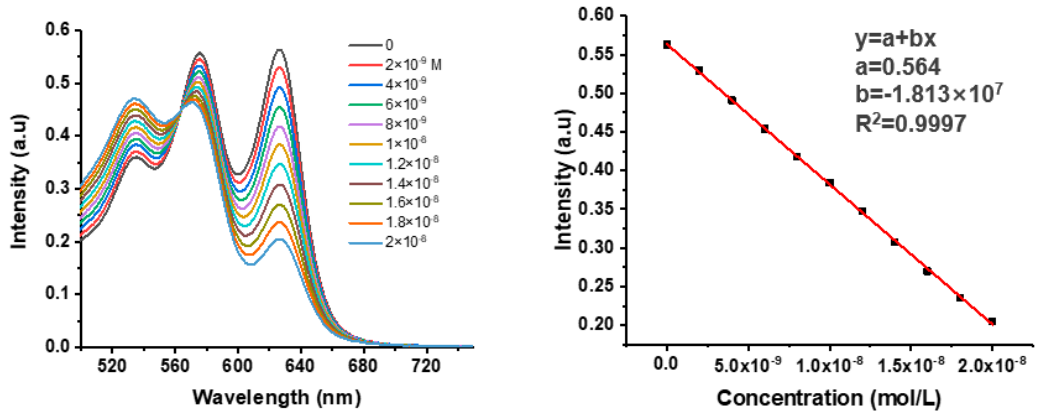


**Figure S4.** Detection of spermine using UV-vis absorption-based sensing assay

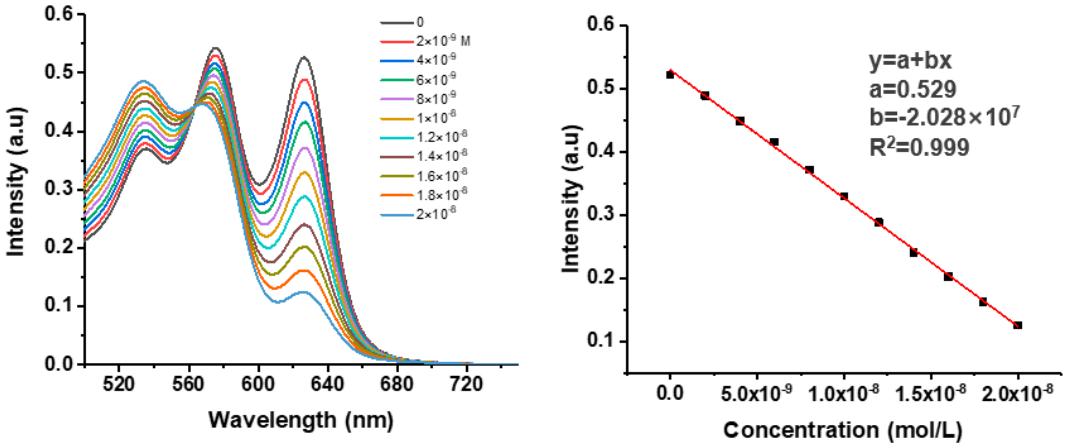


**Figure S5.** Detection of aniline using UV-vis absorption-based sensing assay

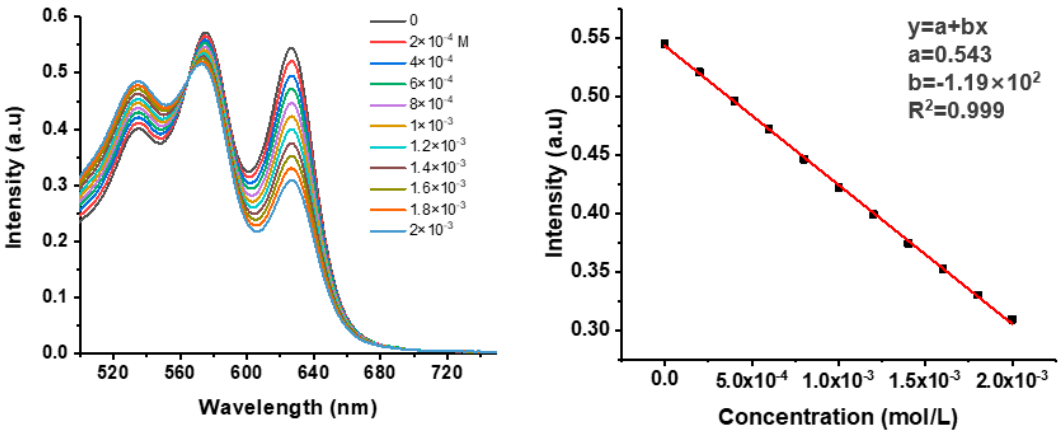


**Figure S6.** Detection of pyrrole using UV-vis absorption-based sensing assay

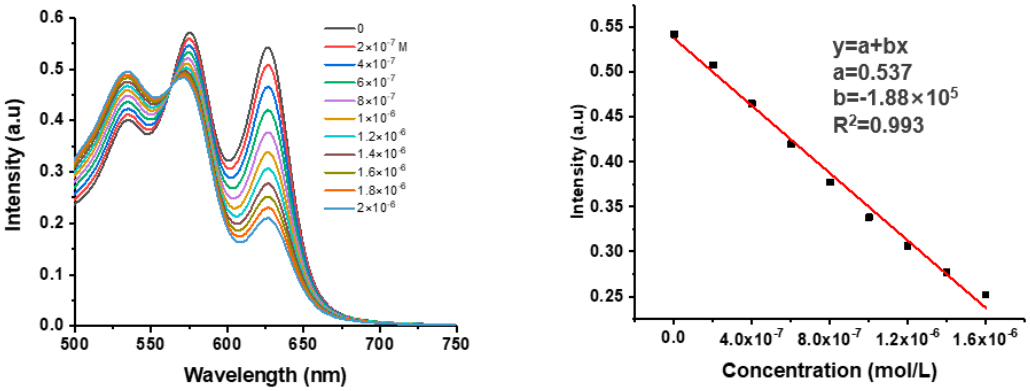


**Figure S7.** Detection of imidazole using UV-vis absorption-based sensing assay

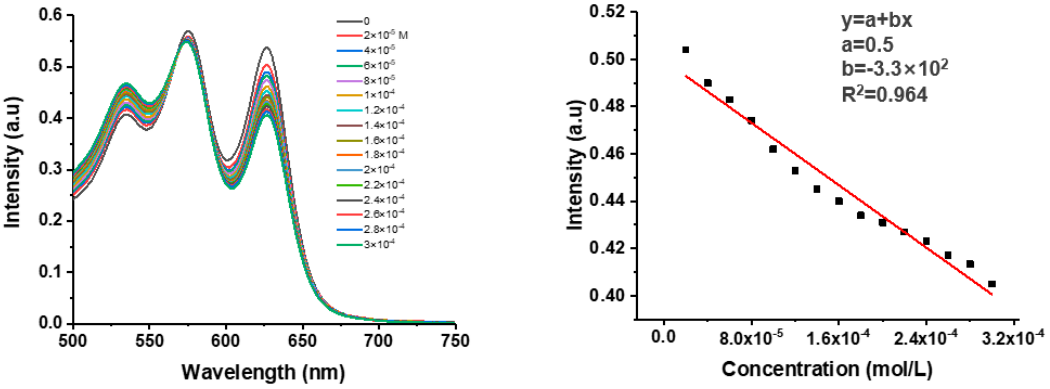


**Figure S8.** Detection of purine using UV-vis absorption-based sensing assay

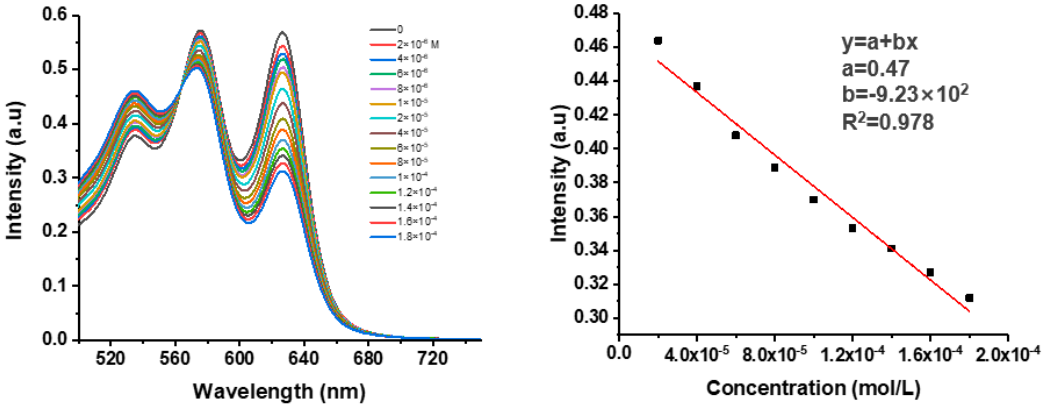


**Figure S9.** Detection of quinoline using UV-vis absorption-based sensing assay

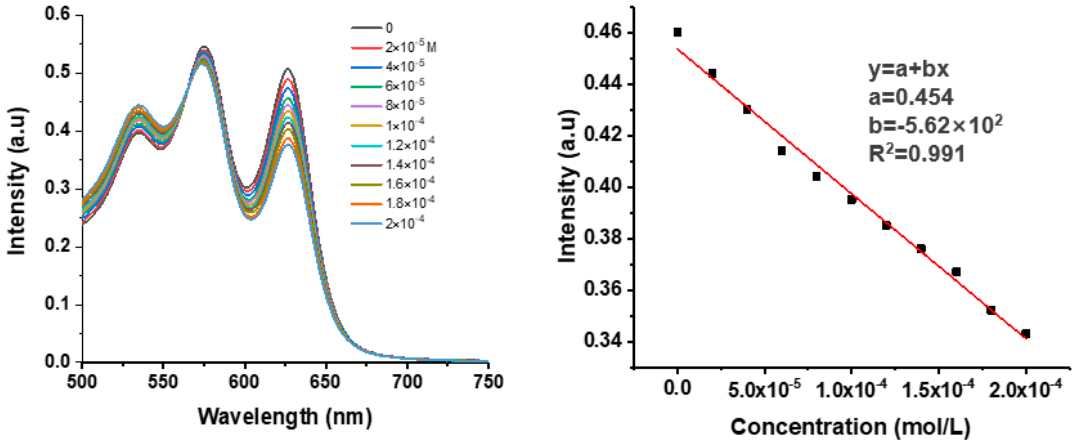


**Figure S10.** Detection of indole using UV-vis absorption-based sensing assay

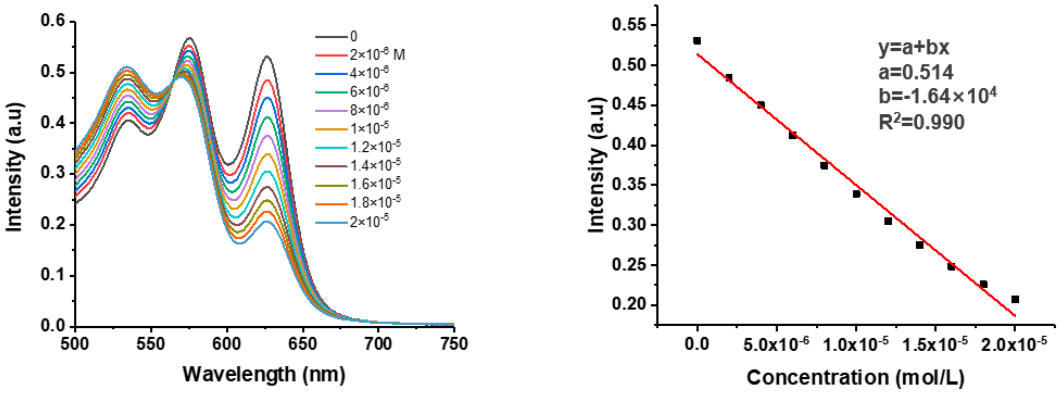


**Figure S11.** Detection of tetracycline using UV-vis absorption-based sensing assay

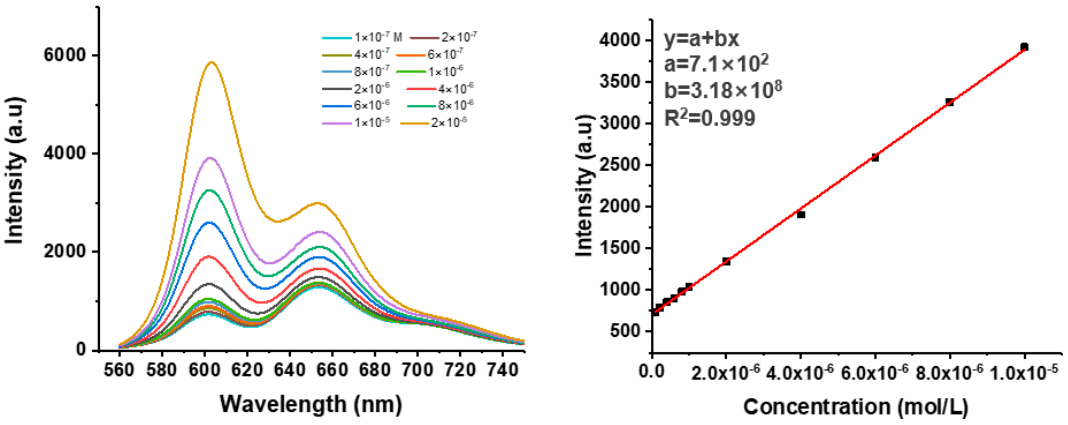


**Figure S12.** Detection of butylamine using PL-based sensing assay

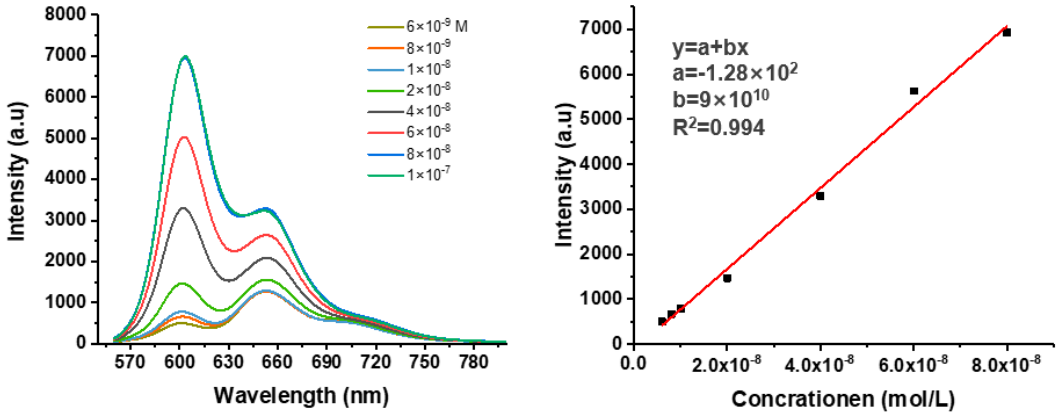


**Figure S13.** Detection of spermine using PL-based sensing assay

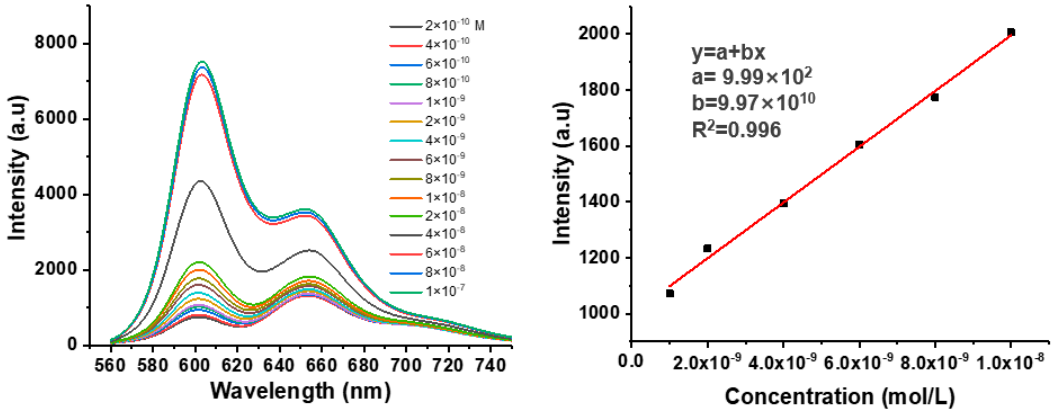


**Figure S14.** Detection of aniline using PL-based sensing assay

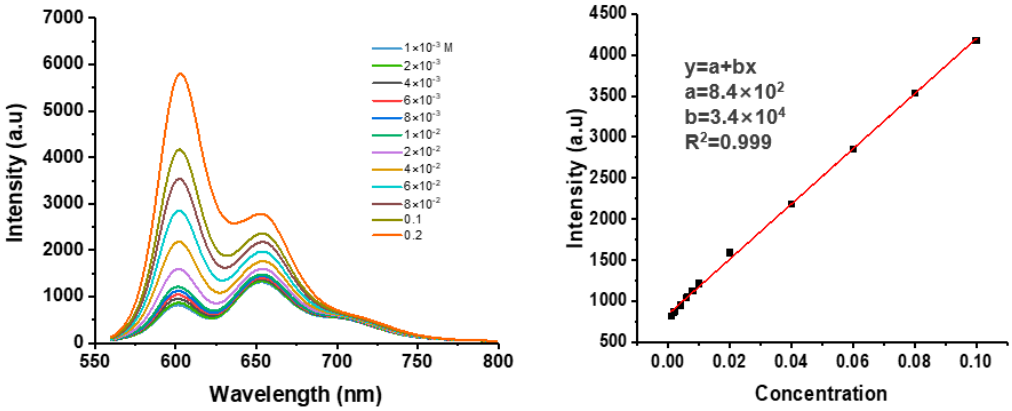


**Figure S15.** Detection of pyrrole using PL-based sensing assay

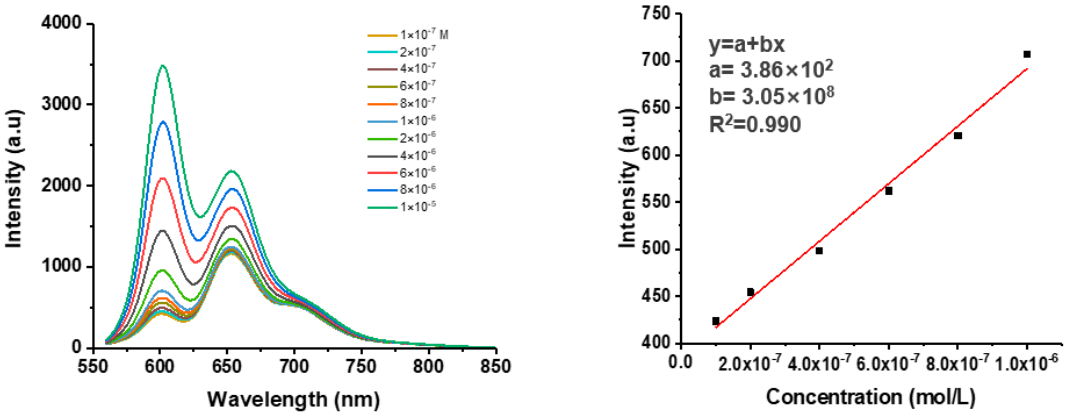


**Figure S16.** Detection of imidazole using PL-based sensing assay

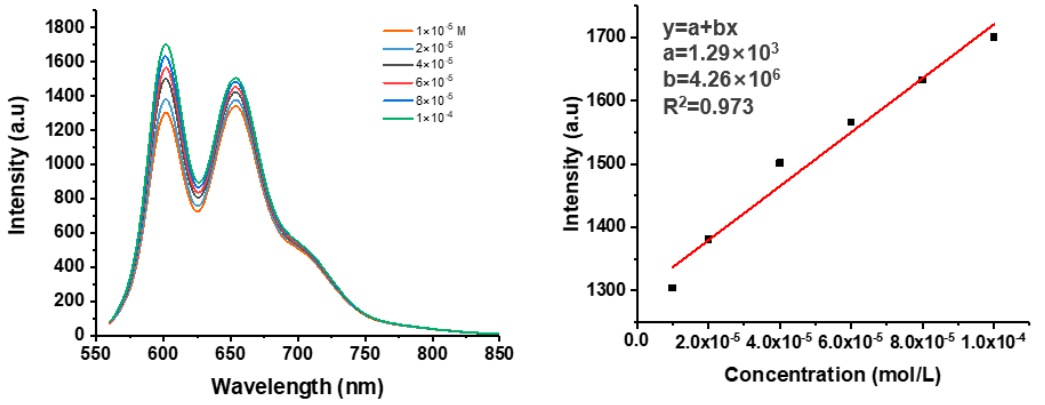


**Figure S17.** Detection of purine using PL-based sensing assay

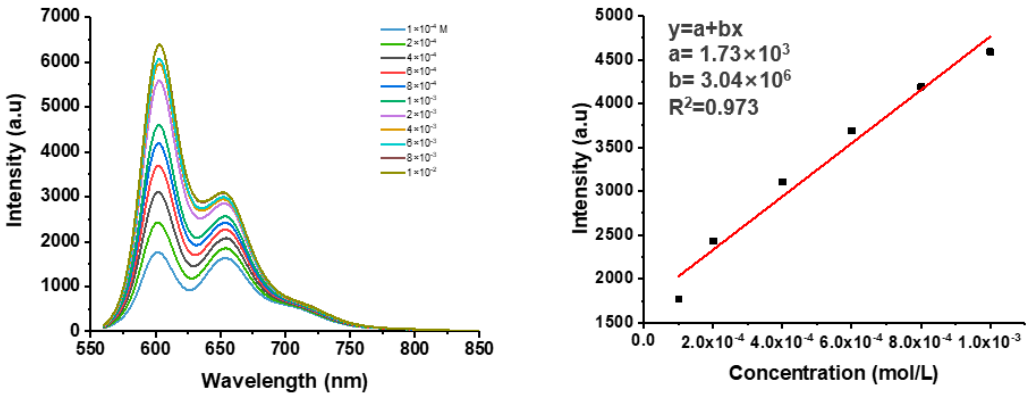


**Figure S18.** Detection of quinoline using PL-based sensing assay

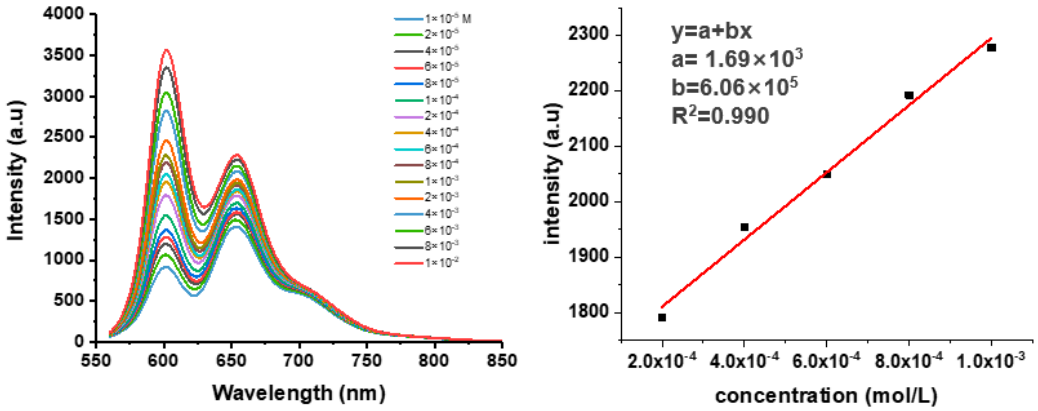


**Figure S19.** Detection of indole using PL-based sensing assay

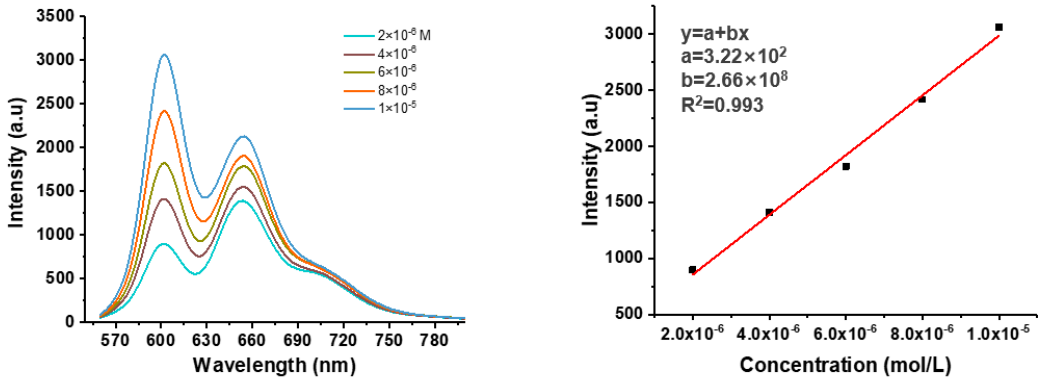


**Figure S20.** Detection of tetracycline using PL-based sensing assay

**Table S1**. Summary of differences between calculated values and the actual values in percentage (Diff. %) of UV-vis absorption- and PL-based assays for the detection of various NCOBs

| NCOBs[a] | Diff. % (UV-Vis) | | | Diff. % (PL) | | |
|---|---|---|---|---|---|---|
| butylamine | 0.4 uM | 1.4 uM | 2.2 uM | 0.15uM | 5.0 uM | 9 uM |
| | 1.6% | 0.6% | 0.8% | 9.7% | 5% | 0.4% |
| spermine | 3 nM | 9 nM | 17 nM | 7 nM | 25 nM | 70 nM |
| | 1.1% | 0.7% | 0.9% | 1.2% | 4.4% | 1.8% |
| aniline | 3 nM | 11 nM | 17 nM | 1.5 nM | 5 nM | 9 nM |
| | 3.6% | 0.9% | 3.8% | 8.9% | 2.7% | 7% |
| pyrrole | 0.3 mM | 1.1 mM | 1.7 mM | 1.5 mM | 50 mM | 90 mM |
| | 3.7% | 0.7% | 1.2% | 9.7% | 3.8% | 4.8% |
| imidazole | 0.3 uM | 0.9 uM | 1.5 uM | 0.15 uM | 5 uM | 9 uM |
| | 1.1% | 0.7% | 3.4% | 4.5% | 6.2% | 4.7% |
| pyridine | 3 nM | 9 nM | 17 nM | 1.5 nM | 25 nM | 50 nM |
| | 3.9% | 0.26% | 2.3% | 9.8% | 8.3% | 2.2% |
| purine | 0.05 mM | 0.15 mM | 0.27 mM | 15 uM | 50 uM | 90 uM |
| | 5.8% | 8.9% | 8.3% | 9.7% | 3.6% | 4.7% |
| quinoline | 30 uM | 90 uM | 170 uM | 0.15 mM | 0.5 mM | 0.9 mM |
| | 8.3% | 3.5% | 4.5% | 7.2% | 5.2% | 3% |
| indole | 30 uM | 90 uM | 170 uM | 0.3 mM | 0.6 mM | 0.9 mM |
| | 6.7% | 2.8% | 5.7% | 9.5% | 2.3% | 2.6% |
| lysine | 1.5 uM | 5.5 uM | 1.7 uM | 0.25 uM | 9 uM | 15 uM |
| | 0.68% | 1.57% | 1.99% | 9.5% | 5.5% | 3% |
| tetracycline | 3 uM | 11 uM | 17 uM | 3 uM | 6 uM | 9 uM |
| | 5.7% | 4.1% | 1.9% | 3.7% | 5.5% | 3.3% |

[a] for each NCOBs, top row presented are the actual concentrations of the NCOBs; and the bottom row presented are the differences in percentage of the calculated values from the calibration curves versus the actual values.

**Table S2.** Comparison of the performance of NCOBs sensing reported in this work to that of prior art.

| | NCOBs | LOD [a] (**this work**)[b] | LOD [a] (**prior art**)[c] | Ref. |
|---|---|---|---|---|
| 1 | butylamine | $5.50\times10^{-2}$ uM | 18 uM | [1] |
| 2 | spermine | 0.50 nM | 1.75 nM | [2] |
| 3 | aniline | 0.53 nM | 6.8 uM | [3] |
| 4 | pyrrole | 0.12 mM | 3.5 uM | [4] |
| 5 | imidazole | 74 nM | 2.65 nM | [5] |
| 6 | pyridine | 0.68 nM | 0.21 uM | [6] |
| 7 | purine | 12.4 uM | 6 uM | [7] |
| 8 | quinoline | 15 uM | - | - |
| 9 | indole | 25 uM | - | - |
| 10 | lysine | 0.20 uM | 19 uM | [8] |
| 11 | tetracycline | 0.20 uM | 5.6 nM | [9] |

[a]LOD, limit of detection (3σ). [b]the results listed here are the best ones achieved in this work from either UV-Vis- or PL-based sensing. [c]only best performance assays found in literature are listed here, which means the work listed here have the lowest LOD among all the work reported.

**References**


1. Yang, X.; Wang, Y.; Fu, H.; Wang, W.; Han, D.; An, X. Experimental and theoretical study on the excellent amine-sensing performance of Au decorated WO3 needle-like nanocomposites. *Mater. Chem. Phys.* **2019**, *234*, 122–132.
2. Bhamore, J.R.; Murthy, Z.; Kailasa, S.K. Fluorescence turn-off detection of spermine in biofluids using pepsin mediated synthesis of gold nanoclusters as a probe. *J. Mol. Liq.* **2019**, *280*, 18–24.
3. Feng, H.-J.; Xu, L.; Liu, B.; Jiao, H. Europium metal–organic frameworks as recyclable and selective turn-off fluorescent sensors for aniline detection. *Dalton Trans.* **2016**, *45*, 17392–17400.
4. Park, S.; Lee, S.-Y. Photoluminescent microrods from the self-assembly of a biomimetic molecule: Application for the optical detection of pyrrole. *Sens. Actuators B*. **2014**, *202*, 690–698.
5. Manshaei, F.; Bagheri, H.; Eshaghi, A. Turn-off chelation-enhanced fluorescence sensing of carbon dot-metallic deep eutectic solvent by imidazole-based small molecules. *Sens. Actuators B* **2021**, *344*, 130228.
6. Ahmed, H.M.; Ghali, M.; Zahra, W.K.; Ayad, M. Optical sensing of pyridine based on green synthesis of passivated carbon dots. *Mater. Today Proc.* **2020**, *33*, 1845–1848.
7. Salve, M.; Amreen, K.; Rajurkar, P.; Pattnaik, P. K.; Goel, S. Miniaturized Disposable Buckypaper-Polymer Substrate Based Electrochemical Purine Sensing Platform. *ECS J. Solid State*

*Sci. Technol.* **2020**, *9*, 101009.

8. Pandey, S.P.; Singh, P.K. A polyelectrolyte based ratiometric optical sensor for arginine and lysine. *Sens. Actuators B* **2020**, *303*, 127182.
9. Velmurugan, S.; Zhi-Xiang, L.; Yang, T. C.; Juan, J. C. Rational design of built-in stannic oxide-copper manganate microrods p-n heterojunction for photoelectrochemical sensing of tetracycline. *Chemosphere* **2021**, *271*, 129788.